

Design and synthesis of intramolecular hydrogen bonding systems. Their application in metal cation sensing based on excited-state proton transfer reaction

Kun-Chan Wu,^a Yu-Shan Lin,^a Yu-Shan Yeh,^a Chun-Yen Chen,^a Moawia O. Ahmed,^a Pi-Tai Chou^{a,*} and Yung-Son Hon^{b,*}

^aDepartment of Chemistry, National Taiwan University, Taipei 106, Taiwan

^bDepartment of Chemistry and Biochemistry, National Chung Cheng University, Chia-Yi 621, Taiwan

Received 14 July 2004; revised 22 September 2004; accepted 24 September 2004

Available online 18 October 2004

Abstract—We reported the design and synthesis of a new type of metal-cation probes, 3-hydroxy-4-(1,4,7,10-tetraoxa-13-azacyclopentadec-13-ylmethyl)naphthalene-2-carbaldehyde (**1a**) and its single hydrogen-bond analogue 1-(1,4,7,10-tetraoxa-13-azacyclopentadec-13-ylmethyl)-2-naphthol (**2a**), in which 1-aza-15-crown-5 ether in combination with the naphthol oxygen acts as a receptor, while the mechanism of excited-state intramolecular proton transfer (ESIPT) is exploited as a signal transducer. The association constant of $(2.5 \pm 0.5) \times 10^4$, $(3.8 \pm 0.4) \times 10^4$, $(5.5 \pm 0.5) \times 10^3$ and $(1.2 \pm 0.3) \times 10^4 \text{ M}^{-1}$ for the formation of **1a**/ Na^+ , **1a**/ Ca^{2+} , **2a**/ Na^+ and **2a**/ Ca^{2+} complexes, respectively, in CH_3CN plus drastic fluorescence changes due to the fine-tuning of ESIPT reaction upon complexation, lead **1a** and **2a** to be highly sensitive fluorescent sensors. The results add a new class into the category of metal-cation probes, with the perspective of designing ESIPT systems capable of sensing bio-analytes.

© 2004 Elsevier Ltd. All rights reserved.

1. Introduction

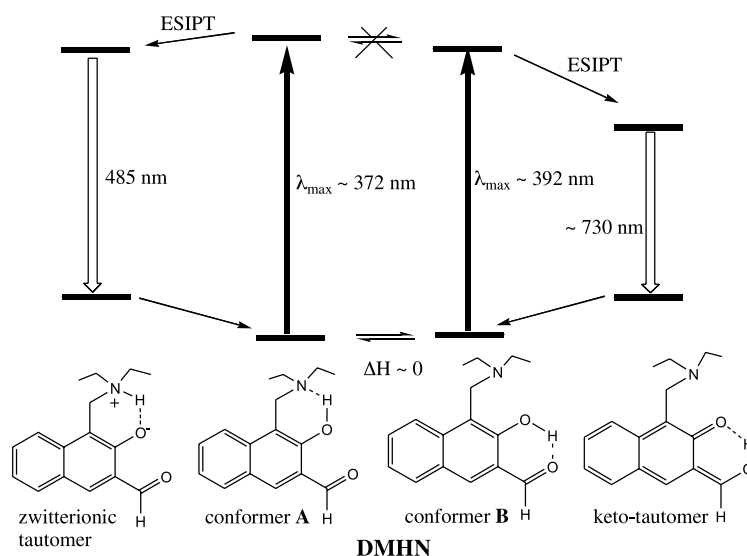
Due to its importance in fundamental research, the excited state intramolecular proton transfer (ESIPT) process has received considerable attention.¹ The ESIPT reaction generally incorporates transfer of a hydroxyl (or amino) proton to the carbonyl oxygen (or pyridinic nitrogen) through a pre-existing six or five membered ring hydrogen bonding (HB) configuration. The resulting proton-transfer tautomer, which generally possesses a vast difference in electronic configuration from its corresponding normal species, exhibits a large Stokes shifted fluorescence. This unusual photophysical property has led to versatile applications such as the development of laser dyes,^{2,3} probes for solvation environments,^{4,5} ultraviolet stabilizers⁶ and radiation hard-scintillator counters,⁷ etc.

Recently, we have applied 1-[(diethylamino)methyl]-3-hydroxy-2-naphthaldehyde (DMHN) possessing dual HB

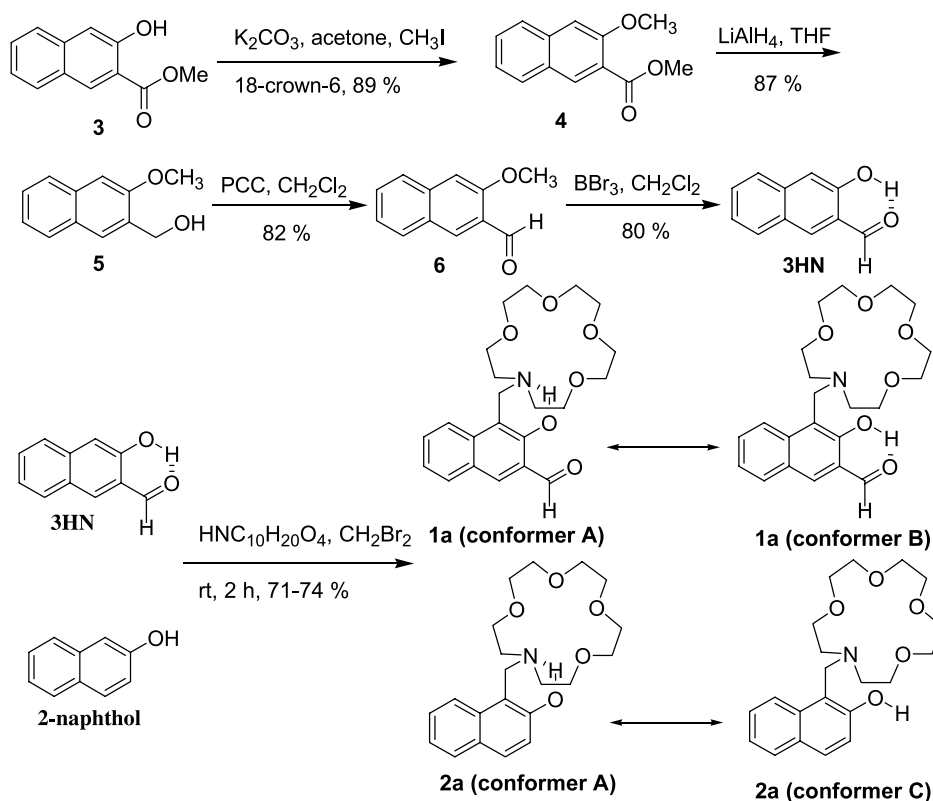
sites (conformers **A** and **B**, see Scheme 1) to study the competitive ESIPT dynamics.⁸ Despite a near degeneracy in the ground electronic state, conformers **A** and **B** undergo entirely different ESIPT dynamics, resulting in a zwitterion ($\lambda_{\text{max}} \sim 485 \text{ nm}$) and a keto-tautomer ($\lambda_{\text{max}} \sim 730 \text{ nm}$) emission, respectively. From the application viewpoint, one intriguing concept is to design ESIPT systems capable of capturing analytes and selectively blocking one HB site. The result may drastically alter the ESIPT pathway, and the associated photophysics can thus be exploited as a new type of sensor for molecule/metal-ion recognition. On this basis, we have designed 3-hydroxy-4-(1,4,7,10-tetraoxa-13-azacyclopentadec-13-ylmethyl)naphthalene-2-carbaldehyde (**1a**) and its single HB analogue 1-(1,4,7,10-tetraoxa-13-azacyclopentadec-13-ylmethyl)-2-naphthol (**2a**). **1a** and **2a** were synthesized from the condensation between 3-hydroxy-naphthalene-2-carbaldehyde (3HN) (or 2-naphthol for **2a**) and 1-aza-15-crown-5 ether via a modified Mannich reaction depicted in Scheme 2, in which 3HN was prepared from the reduction of 3-hydroxy-2-naphthoic acid methyl ester. Both prove to be highly sensitive fluorescent sensors based on the mechanism incorporating metal cation fine-tuning ESIPT reaction, adding a new class into the category of metal-cation probes.^{9,10}

Keywords: Hydrogen bonding; Metal-cation probes; Excited state intramolecular proton transfer reaction; Receptors.

* Corresponding authors. Tel.: +866 2 2363 0231x3988; fax: +886 2 2369 5208 (P.T.C.); e-mail addresses: chop@ntu.edu.tw; cheysh@ccu.edu.tw



Scheme 1. The proposed competitive ES IPT mechanism for DMHN in aprotic solvents.⁸ It should be noted that the rate of interconversion between conformers **A** and **B** in the excited state is too slow to compete with the proton transfer process. Thus, each hydrogen-bonding conformer undergoes independent ES IPT process.



Scheme 2. The synthetic scheme for compounds **1a** and **2a**, and their possible conformers.

2. Experimental

2.1. General

All reactions were performed under nitrogen atmosphere. Solvents were distilled from appropriate drying agents prior to use. Commercially available reagents were used without further purification unless otherwise stated. All reactions were monitored by TLC with Macherey-Nagel pre-coated

glassic sheets (0.20 mm with fluorescent indicator UV₂₅₄). Compounds were visualized with UV light at 254 and 365 nm. Flash column chromatography was carried out using silica gel from Merck (230–400 mesh). ¹H NMR and ¹³C NMR in CDCl₃ were recorded using a Varian (Unity Plus 400) spectrometer at 400 and 100 MHz, respectively. FAB-mass spectroscopy were collected on a JMS-700 double focusing mass spectrometer (JEOL, Tokyo, Japan) with a resolution of 3000 and 8000 for LR and HR

FAB-mass spectra. The source accelerating voltage was operated at 10 kV with Xe gun for FAB-mass spectra, using 3-nitrobenzyl alcohol as matrix.

2.1.1. 3-Methoxy-naphthalene-2-carboxylic acid methyl ester (4). To a suspension of potassium carbonate (2.7 g, 19.8 mmol) in acetone (10 mL) was added 2-hydroxy-3-naphthoic acid methyl ester (2.0 g, 9.9 mmol) and catalyst amount of 18-crown-6 ether (0.3 g, 1.0 mmol), followed by addition of methyl iodide (2.1 g, 14.9 mmol) under nitrogen. The reaction mixture was subjected to reflux for 12 h. The mixture was cooled and the solvent was removed via reduced pressure. The product was then extracted with CH_2Cl_2 . Subsequently, the organic layer was dried with MgSO_4 and filtered, and the solvent was removed in vacuum. The residue was purified by column chromatography (eluent: EtOAc/hexane (1:10 v/v)), yielding compound **4**, (1.9 g, 89%). ^1H NMR (CDCl_3 , 400 MHz) δ 3.9 (s, 3H), 3.98 (s, 3H), 7.18 (s, 1H), 7.34 (td, $J=8.0, 1.2$ Hz, 1H), 7.50 (td, $J=8.0, 1.2$ Hz, 1H), 7.72 (d, $J=8.4$ Hz, 1H), 7.79 (d, $J=8.0$ Hz, 1H); ^{13}C NMR (CDCl_3 , 100 MHz) δ 52.3 (CH_3), 56.0 (CH_3), 106.7 (CH), 114.9 (C), 121.6 (C), 124.3 (CH), 126.3 (CH), 127.4 (C), 128.3 (CH), 128.5 (CH), 132.6 (CH), 135.9 (C), 155.5 (C), 166.5 (C); IR (neat) 3062, 2956, 2837, 1732, 1640, 1590, 1507, 1470, 1428, 1337 cm^{-1} ; FAB-MS m/z (rel intensity) 217 ($\text{M}^+ + 1$, 100%); HRMS (FAB) Calcd for $\text{C}_{13}\text{H}_{12}\text{O}_3$ 216.0786, found 216.0788.

2.1.2. (3-Methoxy-naphthalen-2-yl)-methanol (5). To a suspension of LiAlH_4 (0.7 g, 17.13 mmol) in dry THF (40 mL) was added 3-Methoxy-naphthalene-2-carboxylic acid methyl ester (1.9 g, 8.7 mmol) in dry THF (10 mL) in ice bath. The mixture was stirred at room temperature for 6 h. The reaction was then quenched with water. The product extracted from CH_2Cl_2 was washed with water and dried with MgSO_4 . After filtration CH_2Cl_2 was removed by a rotavapor under reduced pressure and the residue was purified by column chromatography (eluent: EtOAc/hexane (1:5 v/v)), affording compound **5** as a white solid (1.4 g, 87%). ^1H NMR (CDCl_3 , 400 MHz) δ 2.10 (s, 1H), 3.96 (s, 3H), 4.81 (s, 2H), 7.11 (s, 1H), 7.33 (td, $J=7.8, 1.0$ Hz, 1H), 7.42 (td, $J=8.0, 1.0$ Hz, 1H), 7.71–7.76 (m, 3H); ^{13}C NMR (CDCl_3 , 100 MHz) δ 55.4 (CH_2), 62.5 (CH_3), 105.1 (CH), 123.8 (CH), 126.2 (CH), 126.3 (CH), 127.4 (CH), 127.5 (CH), 128.5 (C), 130.3 (C), 134.0 (C), 155.7 (C); IR (neat) 3590, 3406, 3058, 2952, 1644, 1608, 1512, 1465, 1436, 1401, 1340 cm^{-1} ; FAB-MS m/z (rel intensity) 188 (M^+ , 100%); HRMS (FAB) Calcd for $\text{C}_{12}\text{H}_{12}\text{O}_2$ 188.0837, found 188.0839.

2.1.3. 3-Methoxy-naphthalene-2-carbaldehyde (6). A solution of (3-methoxy-naphthalen-2-yl)-methanol (1.3 g 6.7 mmol) in CH_2Cl_2 was added dropwise at 0 °C to a mixture of pyridinium chlorochromate (PCC, 2.2 g 10.0 mmol), sodium acetate (0.8 g 10.0 mmol) and 4 Å molecular sieve (2.2 g) in CH_2Cl_2 . The mixture was stirred for 40 min under inert atmosphere. The solvent was removed under reduced pressure, and the residue was dissolved in ether and filtered. The product was purified by column chromatography. Elution with EtOAc/hexane (1:10 v/v) afforded compound **6** as yellow oil (1.0 g, 82%). ^1H NMR (CDCl_3 , 400 MHz) δ 4.01 (s, 3H), 7.17 (s, 1H), 7.36 (td, $J=8.0, 1.0$ Hz, 1H), 7.52 (td, $J=8.0, 1.0$ Hz,

1H), 7.72 (d, $J=8.0$ Hz, 1H), 7.86 (d, $J=7.6$ Hz, 1H), 8.34 (s, 1H), 10.55 (s, 1H); ^{13}C NMR (CDCl_3 , 100 MHz) δ 55.8 (CH_3), 106.1 (CH), 124.3 (CH), 125.3 (C), 126.2 (CH), 127.4 (C), 128.8 (CH), 129.5 (CH), 130.6 (CH), 137.1 (C), 157.0 (C), 189.4 (CH); IR (KBr) 3064, 2994, 2880, 1700, 1632, 1602, 1470, 1434, 1406, 1346 cm^{-1} ; FAB-MS m/z (rel intensity), 187 ($\text{M}^+ + 1$, 100%); HRMS (FAB) Calcd for $\text{C}_{12}\text{H}_{10}\text{O}_2$ 186.0681, found 186.0684.

2.1.4. 3-Hydroxy-naphthalene-2-carbaldehyde (3HN). Under inert atmosphere, a solution of BBr_3 (0.52 g, 3.2 mmol) in anhydrous CH_2Cl_2 (5 mL) was added at 0 °C to a solution of 3-methoxynaphthalene-2-carbaldehyde (0.5 mg, 2.7 mmol) in anhydrous CH_2Cl_2 (5 mL). The mixture was stirred at room temperature for 1 h, and then the reaction was quenched with 1 N NaHCO_3 aqueous solution. The product was extracted with CH_2Cl_2 , and the resulting organic layers were dried with MgSO_4 . After evaporation of the solvent under reduced pressure, the crude mixture was purified by column chromatography (eluent: EtOAc/hexane (1:20 v/v)), yielding 3HN in 0.37 mg (80%). ^1H NMR (CDCl_3 , 400 MHz) δ 7.23 (s, 1H), 7.36 (t, $J=8.4$ Hz, 1H), 7.55 (t, $J=8.4$ Hz, 1H), 7.70 (d, $J=8.4$ Hz, 1H), 7.85 (d, $J=8.4$ Hz, 1H), 8.13 (s, 1H), 10.06 (s, 1H), 10.30 (s, 1H); ^{13}C NMR (CD_3OD , 100 MHz) δ 111.9 (CH), 122.1 (C), 124.3 (CH), 126.6 (CH), 127.3 (C), 129.2 (CH), 130.1 (CH), 137.7 (CH), 138.0 (C), 155.6 (C), 196.4 (CH); IR (KBr) 3256, 3064, 2985, 2856, 1674, 1518, 1458, 1417, 1388, 1358, 1308 cm^{-1} ; FAB-MS m/z (rel intensity) 172 (M^+ , 100%); HRMS (FAB) Calcd for $\text{C}_{11}\text{H}_8\text{O}_2$ 172.0524, found 172.0528.

2.1.5. 3-Hydroxy-4-(1,4,7,10-tetraoxa-13-azacyclopentadec-13-ylmethyl)naphthalene-2-carbaldehyde (1a). A mixture of 1-aza-15-crown-5 ether (0.6 g, 2.8 mmol) and dibromomethane (1.1 g, 11.4 mmol) was stirred at room temperature for 4 h under inert atmosphere. A solution containing 3-hydroxy-naphthalene-2-carbaldehyde (0.1 g, 0.71 mmol) in CH_2Cl_2 (2 mL) was added and the mixture was stirred at room temperature for 6 h. The solvent was removed under reduced pressure, and the residue was dissolved in diethyl ether and filtered. The product was purified by column chromatography (eluent: methanol/dichloromethane (2:98 v/v)), yielding compound **1a** as yellow oil (203.1 mg, 0.5 mmol, 71%). ^1H NMR (CDCl_3 , 400 MHz) δ 2.90 (t, $J=5.2$ Hz, 4H), 3.60–3.73 (m, 16H), 4.25 (s, 2H), 7.28 (t, $J=8.0$ Hz, 1H), 7.49 (t, $J=8.2$ Hz, 1H), 7.82 (d, $J=8.8$ Hz, 2H), 8.23 (s, 1H), 10.58 (s, 1H); ^{13}C NMR (CDCl_3 , 100 MHz) δ 53.6 (CH_2), 54 (CH_2), 68.7 ($2 \times \text{CH}_2$), 70.3 ($4 \times \text{CH}_2$), 70.8 ($2 \times \text{CH}_2$), 114.1 (C), 121.3 (CH), 123.2 (CH), 124.4 (C), 127.0 (C), 129.0 (CH), 130.4 (CH), 130.9 (CH), 135.9 (C), 157.4 (C), 191.6 (CH); IR (KBr) 3418, 3058, 2873, 1692, 1668, 1630, 1622, 1458, 1399, 1364 cm^{-1} ; FAB-MS m/z (rel intensity) 404 ($\text{M}^+ + 1$, 100%); HRMS (FAB) Calcd for $\text{C}_{22}\text{H}_{29}\text{NO}_6$ 403.1995, found 403.1999; Anal. Calcd for $\text{C}_{22}\text{H}_{29}\text{NO}_6$: C, 65.49; H, 7.24; N, 3.47. Found: C, 65.44; H, 7.29; N, 3.47.

2.1.6. 1-(1,4,7,10-Tetraoxa-13-azacyclopentadec-13-ylmethyl)-2-naphthol (2a). A mixture of 1-aza-15-crown-5 ether (0.6 g, 2.8 mmol) and dibromomethane (1.9 g, 11.0 mmol) was stirred at room temperature for 4 h under inert atmosphere. A solution of 2-naphthol (0.1 g,

0.69 mmol) in CH_2Cl_2 (1 mL) was added and the mixture was stirred at room temperature for 5 h. After removing CH_2Cl_2 under reduced pressure, the residue was dissolved in diethyl ether and filtered. The product was then purified by column chromatography (eluent: ethyl acetate/hexane (1:1 v/v)), yielding compound **2a** (194.1 mg, 74%). ^1H NMR (CDCl_3 , 400 MHz) δ 2.93 (t, $J=5.2$ Hz, 4H), 3.60–3.71 (m, 16H), 4.27 (s, 2H), 7.08 (d, $J=8.8$ Hz, 1H), 7.25 (t, $J=6.8$ Hz, 1H), 7.41 (td, $J=7.6, 1.2$ Hz, 1H), 7.65 (d, $J=8.4, 1.6$ Hz, 1H), 7.72 (d, $J=8.4$ Hz, 1H), 7.82 (d, $J=8.8$ Hz, 1H); ^{13}C NMR (CDCl_3 , 100 MHz) δ 54.3 (CH_2), 54.7 (CH_2), 68.8 (CH_2), 70.3 ($4 \times \text{CH}_2$), 70.7 (CH_2), 111.9 (C), 119.3 (CH), 120.8 (CH), 122.2 (CH), 126.1 (CH), 128.3 (C), 128.7 (CH), 128.0 (CH), 132.6 (C), 156.4 (C); IR (KBr, neat) (cm^{-1}): 3488, 3060, 2874, 1676, 1626, 1602, 1526, 1474, 1410, 1353, 1272, 1238, 1128; FAB-MS m/z (rel intensity) 376 ($\text{M}^+ + 1$, 100%); HRMS (FAB) Calcd for $\text{C}_{21}\text{H}_{29}\text{NO}_5$ 375.2046, found 375.2049; Anal. Calcd for $\text{C}_{21}\text{H}_{29}\text{NO}_5$: C, 67.18; H, 7.79; N, 3.73. Found: C, 65.15; H, 7.76; N, 3.77.

2.2. Spectroscopy and dynamics measurements

Steady-state absorption and emission spectra were recorded by a Hitachi (U-3310) spectrophotometer and an Edinburgh (FS920) fluorimeter, respectively. The excitation light source of the fluorimeter has been corrected by the Rhodamine B spectrum. In addition, the wavelength-dependent characteristics of the monochromator and photomultiplier have been calibrated by recording the scattered light spectrum of the corrected excitation light from a diffused cell in the range of 220–700 nm.

For determining fluorescence quantum yields and relaxation dynamics of the studied compounds, sample solutions were degassed by three freeze-pump-thaw cycles under vigorous stirring condition. Quinine sulfate/1.0 N H_2SO_4 was used as a reference for the quantum yield measurement, assuming a yield of 0.564 with 360 nm excitation. Nanosecond lifetime studies were performed by an Edinburgh FL 900 photon-counting system with a hydrogen-filled/or a nitrogen lamp as the excitation source. Data were analyzed using the nonlinear least squares procedure in combination with an iterative convolution method, which allows partial removal of the instrument time broadening and consequently renders a temporal resolution of ~ 200 ps. A Sutex SP-701 pH-meter was used for the pH titration study.

3. Results and discussion

Similar to that of conformer **A** in DMHN,⁸ the emission of **1a** revealed strong solvent-polarity dependence, being red shifted from 505 nm in cyclohexane to 585 nm in CH_3CN . The spectral shift of the fluorescence upon increasing solvent polarity depends on the difference in permanent dipole moments between ground (μ_g) and excited (μ_e) states, which can be quantitatively expressed based on Lippert equation¹¹ expressed in Eq. 1

$$\tilde{\nu}_f = \tilde{\nu}_f^{\text{vac}} - \left(\frac{2|\tilde{\mu}_e - \tilde{\mu}_g|^2}{hca_0^3} \right) \left(\frac{\epsilon - 1}{2\epsilon + 1} \right) \quad (1)$$

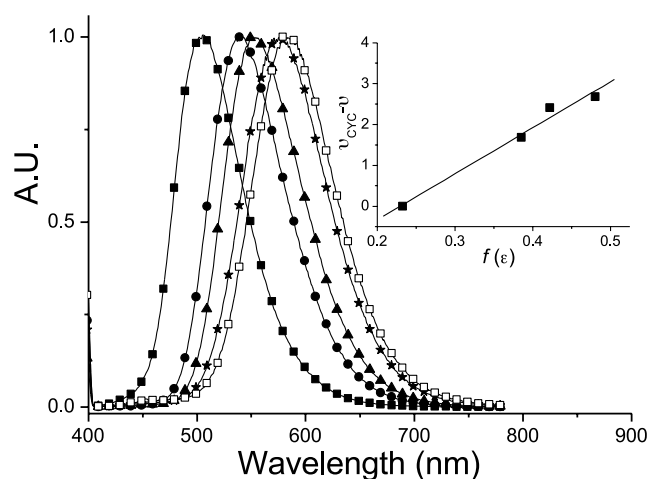


Figure 1. The emission spectra of **1a** in cyclohexane (—■—), benzene (—●—), ethyl acetate (—▲—), dichloromethane (—★—) and acetonitrile (—□—). The emission intensity has been normalized. Insert: the plot of $\tilde{\nu}_f^{\text{cyc}} - \nu_f$ versus $f(\epsilon) = (\epsilon - 1)/(2\epsilon + 1)$ in various solvents.

where a_0 and ϵ denote the cavity radius and solvent dielectric constant, respectively, $\tilde{\nu}_f$ and $\tilde{\nu}_f^{\text{vac}}$ represent the fluorescence peak frequency (in cm^{-1}) in solvent studied and in vacuum, respectively. In this study, $\tilde{\nu}_f^{\text{vac}}$ can be replaced by the peak frequency in cyclohexane ($\tilde{\nu}_f^{\text{cyc}}$) if one neglects the induced dipole interaction. As shown in the insert of Figure 1, the plot of $\tilde{\nu}_f^{\text{cyc}} - \nu_f$ versus $f(\epsilon) = (\epsilon - 1)/(2\epsilon + 1)$ is sufficiently linear, and a slope of as large as $11,200 \text{ cm}^{-1}$ is deduced. a_0 in Eq. 1 was estimated to be 6.4 \AA via the Hartree Fock theories with 6-31G(d',p') basis sets. Accordingly, the change in dipole moment between ground and excited states was deduced to be as large as 17.2 debye.

The results lead us to ascribe the 585 nm emission in CH_3CN to a zwitterionic species resulting from $\text{O-H}\cdots\text{N} \rightarrow \text{O}^- \cdots \text{HN}^+$ ES IPT. In contrast to the existence of conformers **A** and **B** for DMHN, as supported by the significant difference between absorption and excitation spectrum monitored at zwitterion emission,⁸ the excitation spectrum of **1a** in CH_3CN is identical to the absorption spectrum. The results indicate that the $\text{O-H}\cdots\text{N}$ intramolecular HB conformer **A** is the dominant species in **1a**. Further support was given by the lack of resolution of any keto-tautomer emission at > 700 nm predicted according to the ES IPT mechanism in conformer **B** of DMHN.⁸ The more stable conformer **A** in **1a** can qualitatively be rationalized by additional HB interactions between $-\text{O-H}$ and ether oxygens. This viewpoint is also supported by a semi-empirical PM3 approach (see Fig. 2), estimating conformer **A** of **1a** to be energetically lower than conformer **B** by ~ 1.6 kcal/mol. In addition, the dipole moment of 5.52 debye calculated for conformer **A** of **1a** is larger than that of **B** (3.75 debye). Accordingly, it is reasonable to expect the dominant conformer **A** in the strong polar solvent such as CH_3CN .

The corresponding absorption and fluorescence titration spectra in CH_3CN upon the addition of Na^+ to **1a** are shown in Figures 3 and 4, respectively. Table 1 lists the

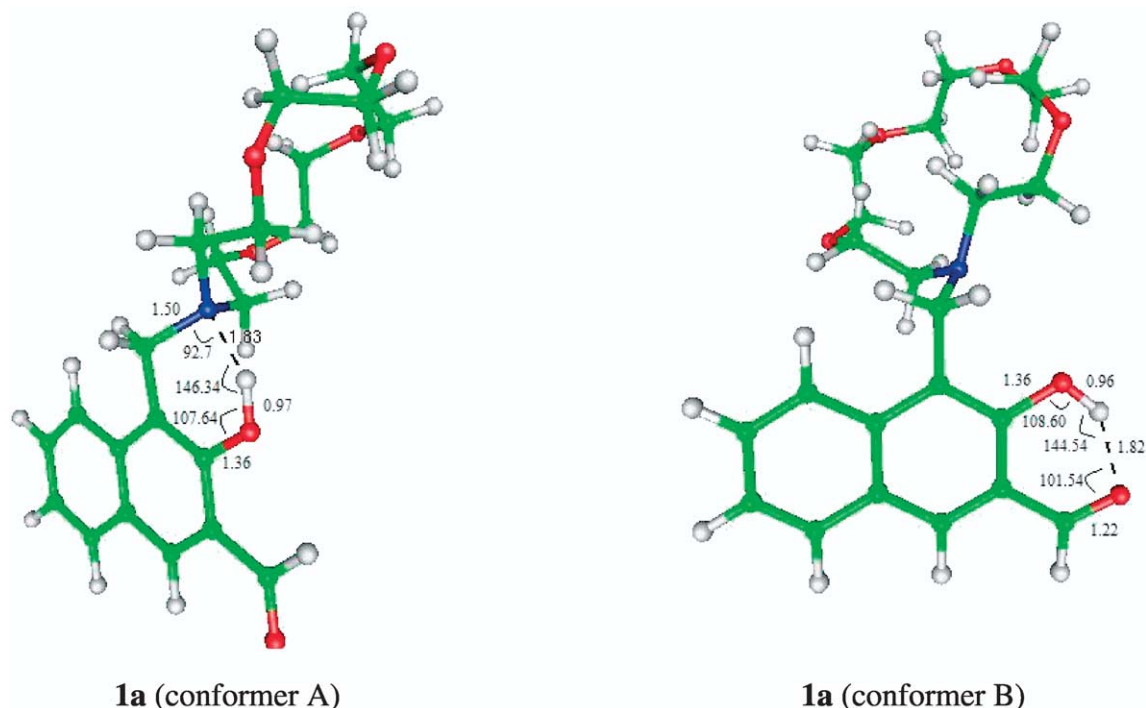


Figure 2. Two geometry-optimized (PM3 method) hydrogen-bonding conformers of **1a**, and the respective critical bond distance (in Å) and angle (in degree) involved in the intramolecular hydrogen bond.

photophysical properties of **1a** and **2a** and their associated metal ion complexes in CH₃CN. Increasing the [Na⁺] led to a hypsochromic shift of the absorption profile, in which the appearance of isosbestic points at ~360 and 315 nm verifies a two-species equilibrium. Thus, the plot of the relationship between the measured absorbance *A* as a function of the added NaClO₄ concentration, *C_g*, can be expressed by Eq. 2¹²

$$\frac{A_0}{A - A_0} = \left(\frac{\varepsilon_M}{\varepsilon_c - \varepsilon_M} \right) \left[\frac{1}{K_a [C_g]} + 1 \right] \quad (2)$$

where ε_M and ε_c are molar extinction coefficients of **1a**

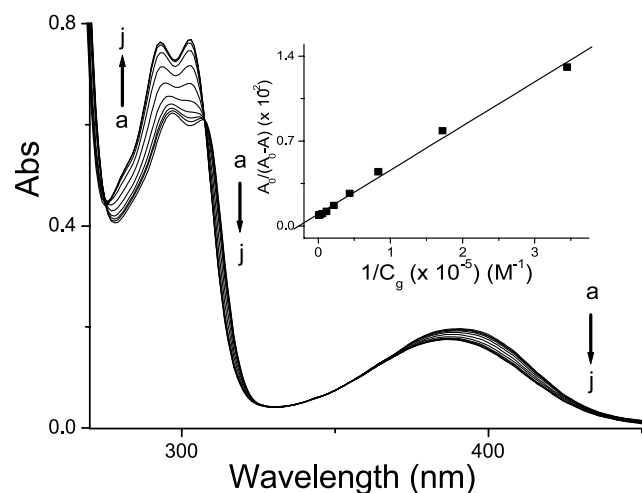


Figure 3. Absorption spectra of **1a** (3.2×10^{-5} M) in CH₃CN by adding NaClO₄ concentrations (*C_g*) of (a) 0, (b) 1, (c) 2, (d) 4, (e) 8, (f) 16, (g) 30, (h) 60, (i) 120, (j) 240 equiv (1 equiv = 2.9×10^{-6} M). Insert: the plot of $A_0/A_0 - A$ against $1/C_g$ at 400 nm.

and **1a**/Na⁺ complex, respectively, at a selected wavelength. *A₀* denotes the absorbance of the free **1a** at that specific wavelength. The 1:1 **1a**/Na⁺ complexation was supported by a straight-line plot for the ratio of absorbance, $A_0/(A_0 - A)$, versus $1/[Na^+]$ throughout the titration (insert of Fig. 3), and an association constant of as high as $(2.5 \pm 0.5) \times 10^4$ M⁻¹ was deduced in CH₃CN.

Drastic changes on the Na⁺ fluorescence titration spectra were also observed, in which the 585 nm zwitterion emission decreased with increasing Na⁺ concentrations (Fig. 4). The relationship between the measured

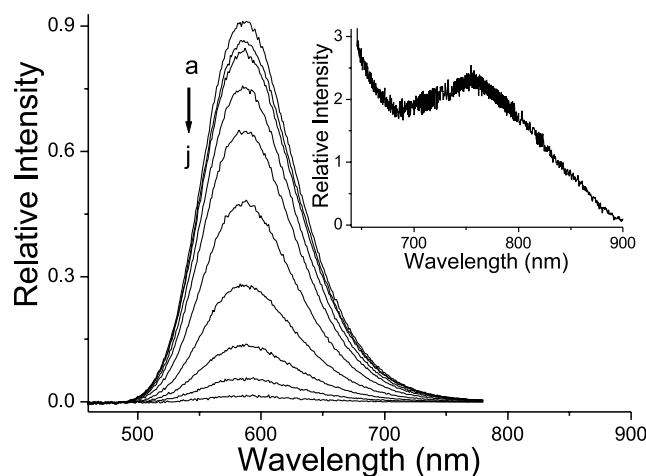


Figure 4. Fluorescence spectra of **1a** (3.2×10^{-5} M) in CH₃CN by adding NaClO₄ concentrations (*C_g*) of (a) 0, (b) 1, (c) 2, (d) 4, (e) 8, (f) 16, (g) 30, (h) 60, (i) 120, (j) 240 equiv (1 equiv = 2.9×10^{-6} M), λ_{ex} : 400 nm. Insert: The spectrum of **1a** at >700 nm by adding 10^{-3} M NaClO₄.

Table 1. The photophysical properties of ion-free **1a** and **2a** and the association constants of various **1a**/metal ion and **2a**/metal ion complexes in CH₃CN

	Absorption λ_{\max} (nm)	Fluorescence λ_{\max} (nm), τ_f	Association constant K_a (M^{-1})	
			Na ⁺	Ca ²⁺
1a	390	585 (4.7 ns), 730 (520 fs)	2.3×10^4	3.8×10^4
2a	327	355 (4.6 ns), 432 (4.3 ns)	5.5×10^3	1.2×10^4

fluorescence intensity F and C_g in a selected wavelength can be expressed by Eq. 3¹²

$$\frac{F_0}{F - F_0} = \frac{\Phi_M \varepsilon_M}{(\Phi_C \varepsilon_C - \Phi_M \varepsilon_M)} \left(\frac{1}{K_a C_g} + 1 \right) \quad (3)$$

where F_0 denotes the fluorescence intensity of free **1a**. Φ_M and Φ_C are fluorescence quantum yields of the free **1a** and complex, respectively, which are assumed to be constant throughout the titration. A linear plot for the ratio of fluorescence intensity, $F_0/(F - F_0)$, versus $1/[Na^+]$ for the 585 nm band reconfirmed the 1:1 complex formation, and K_a was deduced to be $(2.3 \pm 0.3) \times 10^4 M^{-1}$. Upon the addition of $[Na^+]$ of $> 10^{-3} M$, in which $> 99\%$ of **1a**/ Na^+ complex is formed, a weak emission band ($\Phi_f < 10^{-4}$) maximized at ~ 730 nm was observed (see insert of Fig. 4). The mechanism of complexation can thus be rationalized by the rupture of the O–H \cdots N hydrogen bond due to the usage of lone pair electrons on the nitrogen atom upon formation of the **1a**/ Na^+ complex, resulting in switching the intramolecular HB sites from O–H \cdots N (conformer **A**) to O–H \cdots O=C (conformer **B**). ESIPT takes place in the Na^+ /conformer **B** complex, giving rise to a keto-tautomer 730 nm emission.

In contrast to a unique, zwitterionic emission band in **1a**, **2a** exhibits dual emission maximized at 355 (4.6 ns) and 432 nm ($\tau_f = 4.3$ ns) (see Fig. 5). Similar to that assigned for 1-diethylaminomethyl-2-naphthol,¹³ the 432 nm emission can be ascribed to a zwitterion emission resulting from ESIPT. Accordingly, the 355 nm band, being a mirror image

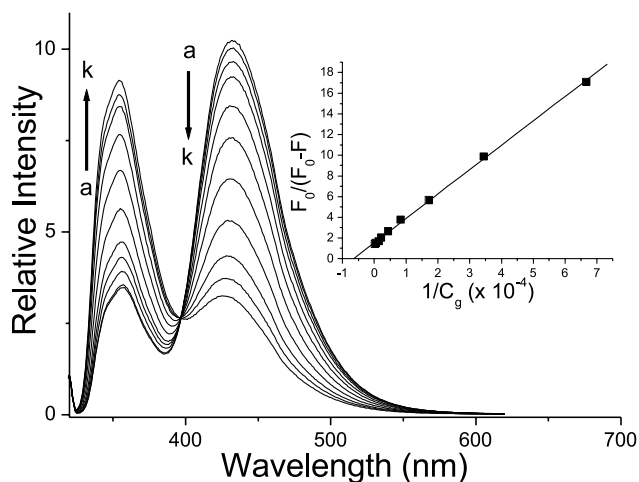


Figure 5. Fluorescence spectra of **2a** ($3.2 \times 10^{-5} M$) in CH₃CN by adding NaClO₄ concentrations (C_g) of (a) 0, (b) 1, (c) 5, (d) 10, (e) 20, (f) 40, (g) 80, (h) 160, (i) 230, (j) 650, (k) 1300 equiv (1 equiv = $2.9 \times 10^{-6} M$). Insert: the plot of $F_0/(F_0 - F)$ against $1/C_g$, λ_{ex} : 320 nm.

with respect to the S_0 – S_1 ($\pi\pi^*$) absorption of **2a**, can be unambiguously ascribed to the emission associated with the normal form of **2a** in that the intramolecular hydrogen bond is ruptured due to the strong solute-solvent polar-polar interaction in CH₃CN. ESIPT is thus prohibited during the lifespan of the excited conformer **C**. It should be noted that the existence of conformer **C** is negligible in **1a** due to its dual HB sites, that is, conformers **A** and **B**, providing an intact intramolecular HB environment free from solvent perturbation.

Titration of **2a** by NaClO₄ revealed a similar hypsochromic absorption shift with that of **1a**, and an association constant of $(5.5 \pm 0.5) \times 10^3 M^{-1}$ was deduced in CH₃CN (not shown here). During titration the 432 nm emission band decreased, accompanied by the increase of a 355 nm normal emission ($\tau_f = 4.6$ ns) with an isoemissive point at 397 nm. The results lead us to conclude the rupture of the O–H \cdots N hydrogen bond on the formation of the **2a**/ Na^+ complex so that ESIPT is prohibited, giving rise to a normal Stokes shifted emission. This is quite different from **1a** in that the conformation of **1a** switches from the OH \cdots N to the OH \cdots O=C site upon **1a**/ Na^+ complexation, resulting in a weak keto-tautomer emission (vide supra). In comparison to **2a**, the ~ 4 -folds larger K_a value in **1a** can be rationalized by the more stable **1a**/ Na^+ complex due to the intramolecular OH \cdots O=C hydrogen bond formation.

Attempts have also been made to titrate DMHN with Na^+ . The results revealed negligible spectral differences, verifying the importance of capping Na^+ with 1-aza-15-crown-5 ether in **1a** and **2a**. Furthermore, within the same range of concentrations, absorption and emission titration remained unchanged on adding K^+ to both **1a** and **2a**, and the results can simply be rationalized by the mismatched sizes between K^+ and 1-aza-15-crown-5 ether.

The absorption and emission spectra of **1a** as a function of the divalent metal ions, for example, Ca^{2+} , in CH₃CN are shown in Figure 6. Upon an increase in $[Ca^{2+}]$, a decrease in the 393 nm absorption band was observed, accompanied

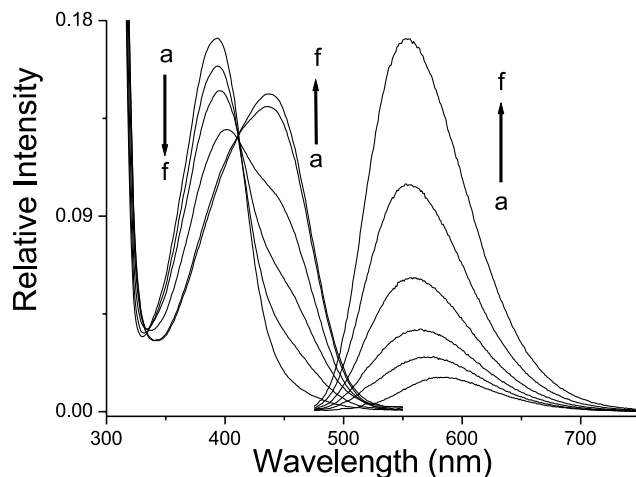


Figure 6. Absorption and emission spectra of **1a** ($3.2 \times 10^{-5} M$) in CH₃CN by adding Ca^{2+} concentrations (C_g): (a) 0, (b) 1, (c) 2, (d) 4, (e) 6, (f) 8, (g) 18, (h) 23, (i) 28, (j) 33 equiv (1 equiv = $2.9 \times 10^{-6} M$), λ_{ex} : 450 nm.

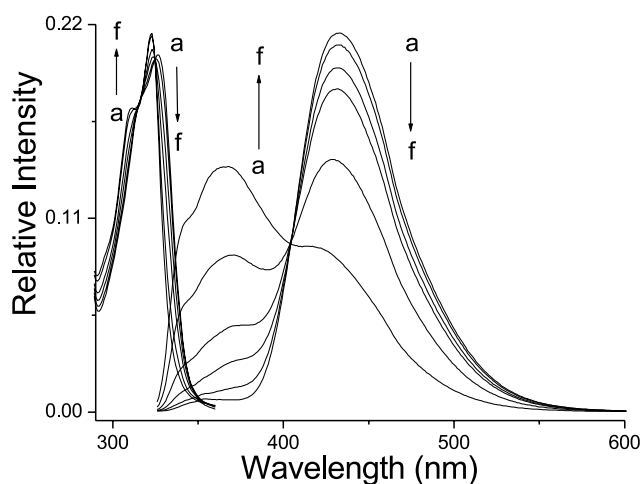


Figure 7. Absorption and emission spectra of **2a** (3.2×10^{-5} M) in CH_3CN by adding Ca^{2+} concentrations ($C_{\text{Ca}^{2+}}$): (a) 0, (b) 2, (c) 4, (d) 6, (e) 10, (f) 15 equiv (1 equiv = 2.9×10^{-6} M). λ_{exc} : 320 nm.

by the gradual increase of a new band maximized at 438 nm and the appearance of an isosbestic point at 412 nm. The straight-line plot of $A_0/(A - A_0)$ versus $1/[\text{Ca}^{2+}]$ confirms a 1:1 **1a**/ Ca^{2+} complexation, and an association constant of $(3.8 \pm 0.4) \times 10^4 \text{ M}^{-1}$ was deduced. Upon 450 nm excitation, the increase of fluorescence intensity as a function of $[\text{Ca}^{2+}]$ was observed, and the emission peak wavelengths shifted from 580 to 560 nm (Fig. 6). During titration, the relaxation dynamics of the entire band could be well fitted by biexponential decay kinetics, and lifetimes were resolved to be 4.7 and 7.1 ns, indicating the existence of two distinct species. Due to its spectral similarity with that of the KOH basified **1a** oxide (in MeOH), the 438 nm absorption band can be assigned to a **1a**/ Ca^{2+} complex absorption, in which the hydroxyl proton is detached to form oxide, along with the nitrogen atom binding to Ca^{2+} , giving rise to a 560 nm ($\tau_f \sim 7.1$ ns) anion emission. In a comparative study, although similar spectral change was observed upon titration of DMHN with Ca^{2+} , the association constant of $(8.0 \pm 0.3) \times 10^3 \text{ M}^{-1}$ is smaller than that of the **1a**/ Ca^{2+} complex by \sim five folds. We thus conclude that in addition to oxide (O^-) and nitrogen atoms, the remaining ether

oxygens in azacrown are also incorporated in the **1a**/ Ca^{2+} complexation. A similar coordination structure has been reported in a $([\text{Ca}(1\text{-aza-15-crown-5 ether})(\text{CH}_3\text{-OH})_2] \text{BPh}_4)$ single crystal.¹⁴

In contrast to the oxy-anion characteristic for the **1a**/ Ca^{2+} complex, drastically different $\text{Ca}(\text{ClO}_4)_2$ titration spectra for **2a** were observed, in which increasing Ca^{2+} resulted in a hypsochromic spectral shift with an appearance of an isosbestic point at 324 nm (Fig. 7). The lack of oxide absorption indicates that the hydroxyl group remains intact in **2a** during the Ca^{2+} titration. This viewpoint is further supported by a decrease of the 435 nm zwitterion emission during the titration, accompanied by an increase of the 360 nm normal emission with an isoemissive point appearing at 405 nm. The difference in capping Ca^{2+} can be qualitatively rationalized by the stronger acidity of the hydroxyl group in **1a** due to the aldehyde (CHO) electron withdrawing property ($\text{p}K_a \sim 6.6$ in **1a** versus ~ 7.7 in **2a** according to the pH titration shown in Fig. 8). The dissimilar binding property is also manifested by the association strength, in which K_a of $(1.2 \pm 0.3) \times 10^4 \text{ M}^{-1}$ for **2a** is smaller than that of **1a** by more than three folds.

4. Conclusion

In conclusion, we have reported the design and synthesis of a new type of metal-cation probes **1a** and **2a**, in which 1-aza-15-crown-5 ether in combination with a hydroxyl group acts as a receptor, while a mechanism of switch or prohibition of ESIPT upon complexation is exploited as the signal transducer. **1a** is superior to **2a** owing to its larger K_a values and metal-ion-selective spectral change. It is thus conceivable to design multiple HB systems capable of sensing bio-analytes based on the ESIPT mechanism. Further work focusing on this issue is currently in progress.

Acknowledgements

We thank the National Science Council for financial support.

References and notes

- (a) Kosower, E. M.; Huppert, D. *Ann. Rev. Phys. Chem.* **1986**, *37*, 127–156. (b) Special Issue *Spectroscopy and Dynamics of Elementary Proton Transfer in Polyatomic Systems*; Firth, D., Barbara, P. F., Trommsdorff, H. P., Eds.; *Chem. Phys.* **1989**, *130*, 349–360. (c) Formosinho, S. F.; Arnaut, L. G. *J. Photochem. Photobiol. A Chem.* **1993**, *75*, 21–48. (d) Scheiner, S. *J. Phys. Chem. A* **2000**, *104*, 5898–5909. (e) Waluk, J. Conformational aspects of intra- and intermolecular excited state proton transfer. In *Conformational Analysis of Molecules in Excited States*; Waluk, J., Ed.; Wiley, 2000. (f) Chou, P. T. *J. Chin. Chem. Soc.* **2001**, *48*, 651–682. (g) Elsaesser, T. Ultrafast excited state hydrogen transfer in the condensed phase. In *Ultrafast Hydrogen Bonding Dynamics and Proton*

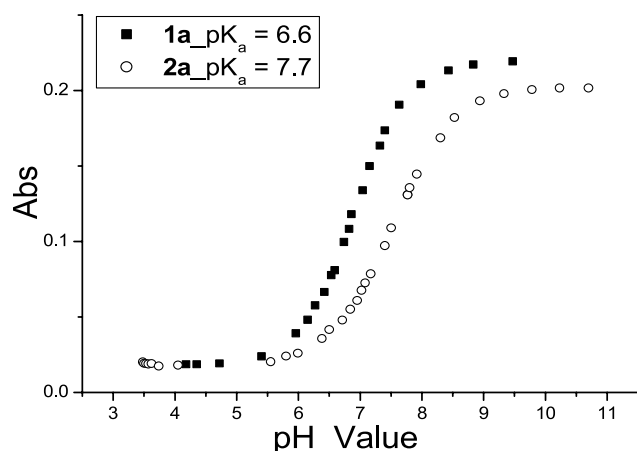


Figure 8. The ground-state pH (NaOH) titration experiment for **1a** (■) and **2a** (●) in water. Data were obtained from the pH dependent absorbance at 450 nm and 350 nm for **1a** and **2a**, respectively.

- Transfer Processes in the Condensed Phase*; Elsaesser, T., Bakker, H. J., Eds.; Kluwer: Dordrecht, 2002.
2. Chou, P. T.; McMorro, D.; Aartsma, T. J.; Kasha, M. *J. Phys. Chem.* **1984**, *88*, 4596–4599.
 3. Acuna, A. V.; Amat, F.; Catalán, J.; Costella, A.; Figuera, J. M.; Munoz, J. M. *Chem. Phys. Lett.* **1986**, *132*, 567–569.
 4. Parsapour, F.; Kelley, D. F. *J. Phys. Chem.* **1996**, *100*, 2791–2798.
 5. Sytnik, A.; Kasha, M. *Proc. Natl. Acad. Sci.* **1994**, *91*, 8627–8630.
 6. Catalán, J.; del Valle, J. C.; Claramunt, R. M.; Sanz, D.; Dotor, J. *J. Lumin.* **1996**, *68*, 165–170.
 7. Renschler, C. L.; Harrah, L. A. *Nucl. Instrum. Methods Phys. Rev.*, *A235*, Sept., *U.S. Patent* **1985**, 635–639.
 8. Wu, K. C.; Cheng, Y. M.; Lin, Y. S.; Yeh, Y. S.; Pu, S. C.; Hu, Y. H.; Yu, J. K.; Chou, P. T. *Chem. Phys. Lett.* **2004**, *384*, 203–209.
 9. (a) For fluorescent Ca^{2+} metal ion chemosensors, see: Mlyamaki, A.; Llopis, J.; Holm, R.; McCarffery, J. A.; Ikurn, M.; Tsien, R. Y. *Nature* **1997**, *388*, 882–887. (b) Arunkumar, E.; Chithra, P.; Ajayaghosh, A. *J. Am. Chem. Soc.* **2004**, *126*, 6590–6598. (c) Yamniuk, A. P.; Nguyen, L. T.; Hoang, T. T.; Vogel, H. J. *Biochemistry* **2004**, *43*, 2558–2568.
 10. Roshal, A. D.; Grigorovich, A. V.; Doroshenko, A. O.; Pivovarenko, V. G. *J. Phys. Chem. A* **1998**, *102*, 5907–5914.
 11. Lakowicz, J. R. *Principles of Fluorescence Spectroscopy*; Plenum: New York, 1999; pp 185–192.
 12. Chou, P. T.; Wu, G. R.; Wei, C. Y.; Cheng, C. C.; Chang, C. P.; Hung, F. T. *J. Phys. Chem. B* **2000**, *104*, 7818–7829. A_0 , F_0 , A and F denote respectively the absorbance and fluorescent intensity of free **1a**, and solution after adding metal ions at a selective wavelength.
 13. Tolbert, L. M.; Nesselroth, S. M. *J. Phys. Chem.* **1991**, *103*, 10331–10336.
 14. Itoh, S.; Kumei, H.; Nagatomo, S.; Kitagawa, T.; Fukuzumi, S. *J. Am. Chem. Soc.* **2001**, *123*, 2165–2175.